Available online at www.sciencedirect.com
SCIENCE DIRECT®
International Journal of Pharmaceutics 308 (2006) 200–204
INTERNATIONAL JOURNAL OF PHARMACEUTICS
www.elsevier.com/locate/ijpharm

Pharmaceutical Nanotechnology

Polymeric nanoparticulate delivery system for Indocyanine green: Biodistribution in healthy mice

Vishal Saxena [a], Mostafa Sadoqi [b], Jun Shao [a,*]

[a] *Department of Pharmacy and Administrative Sciences, College of Pharmacy and Allied Health Professions, St. John's University, 8000 Utopia Parkway, Jamaica, NY 11439, USA*
[b] *Department of Physics, St. John's College of Liberal Arts and Sciences, St. John's University, 8000 Utopia Parkway, Jamaica, NY 11439, USA*

Received 10 June 2005; received in revised form 4 November 2005; accepted 9 November 2005

Abstract

The objective of this study is to investigate the biodistribution of Indocyanine green (ICG) in healthy mice, when delivered through polymeric nanoparticles. The poly(DL-lactic-co-glycolic acid) (PLGA) nanoparticles entrapping ICG were engineered and characterized. The extraction method for ICG recovery from biological samples was developed. The biodistribution of ICG was determined in healthy C57BL/6 mice (female, 10-week old) when delivered through PLGA nanoparticles in comparison to free ICG solution, using a fluorometric assay method. The extraction method for ICG shows efficiency above 80% for various organs and plasma. When nanoparticles were used to deliver ICG, 2–8 times higher concentrations of ICG was deposited in various organs, with 5–10 times higher plasma levels till 4 h, after an i.v. dose as compared to free ICG solution. In conclusion, the nanoparticle formulation significantly increased the ICG concentration and circulation time in plasma as well as the ICG uptake, accumulation and retention in various organs. Overall, this study represents the first step in exploring and establishing the potential of nanoparticles as an ICG-delivery system for use in tumor-diagnosis and photodynamic therapy.

Keywords: Indocyanine green; PLGA nanoparticles; Biodistribution; Tumor-diagnosis; Photodynamic therapy

1. Introduction

Indocyanine green (ICG) is a water-soluble tricarbocyanine dye, which has been approved by the United States Food and Drug Administration for various medical diagnostic applications (Philip et al., 1996; Maarek et al., 2001; Saxena et al., 2003). Recently, much attention has been focused on the potential of ICG as fluorescence contrast agent in diagnostic imaging for early detection of superficial tumors such as of breast and skin cancer (Saxena et al., 2004a,b). Moreover photodynamic therapy using ICG is also a promising method, which is now being evaluated for superficial tumor destruction (Fickweiler et al., 1997; Abels et al., 2000). It has been shown that incubation of tumor cells with ICG and then subsequent irradiation with a diode laser leads to cell killing by photo-oxidation (Fickweiler et al., 1997; Abels et al., 2000). An important motivation for using ICG in above-mentioned studies is its strongest absorption band around 800 nm and its most intense emission around 820 nm. These are the wavelengths for which the blood and other tissues are relatively transparent and the penetration depth of light in biological tissue is the highest (Saxena et al., 2003).

For both tumor-imaging and photodynamic anticancer therapy applications, the delivery of ICG to the tumor site, intracellular uptake of ICG and accumulation and retention in the tumor are the crucial steps. Once injected in blood circulation, all these crucial steps mainly depend upon the protein binding and blood circulation time of ICG. Now, ICG has a very high protein binding in the blood and shows rapid elimination from the body (plasma $t_{1/2}$ = 2–4 min) (Mordon et al., 1998; Desmettre et al., 2000). This leads to low intracellular uptake and minimal accumulation of ICG, at the tumor site, respectively. Thus, these characteristics of ICG are the major limitations in its above-mentioned novel applications in tumor-imaging and anticancer therapy.

Thus, efficient delivery of ICG to the tumor site and its retention at tumor site is required for application of ICG in

* Corresponding author. Tel.: +1 718 990 2510; fax: +1 718 990 6316.
E-mail address: shaoj@stjohns.edu (J. Shao).

0378-5173/$ – see front matter © 2005 Elsevier B.V. All rights reserved.
doi:10.1016/j.ijpharm.2005.11.003

tumor-diagnosis and destruction. For this purpose, an intravenously administrable product/system for ICG having ability for tumor targeting and efficient intracellular uptake will be of great interest. One of the approaches can be ICG delivery to the tumor site and subsequently into the tumor cells through a polymeric nanoparticulate system (Leroux et al., 1996). Now, nanoparticulate delivery systems are associated with enhanced permeation and retention (EPR) effect, which is filtering out of the nanoparticle from the blood stream (in the blood vessel) into the tumor site (due to the leaky vasculature at the tumor site) and subsequently accumulating at that site (Monsky et al., 1999). Thus, the EPR effect provides passive targeting to the tumor site for the nanoparticulate delivery systems. The polymeric nanoparticles containing ICG will thus provide passive tumor targeting of ICG to the tumor site.

In our earlier studies, we have engineered a nanoparticulate formulation for ICG by entrapping ICG within poly(DL-lactic-co-glycolic acid) (PLGA) polymeric matrix (Saxena et al., 2004a,b,c). Also, we have established that these nanoparticles provided efficient aqueous-stability, photo-stability and thermal-stability to ICG (Saxena et al., 2004a). Moreover we have proved that these nanoparticles enhanced the in vitro intracellular uptake of ICG in the tumor cells (Saxena et al., 2005). Now, the main focus of our present study is to characterize the in vivo biodistribution of ICG in healthy animal model, when delivered through PLGA nanoparticles, to access the merit of PLGA nanoparticles as ICG carriers and delivery systems over free ICG solution, for tumor-diagnosis and anticancer therapy.

Thus, studies on development of extraction method of ICG from biological samples and determination of the biodistribution of ICG using PLGA nanoparticles were performed on healthy mice. Also for comparison ICG biodistribution was also determined using free ICG solution. This knowledge of in vivo biodistribution of ICG through PLGA nanoparticles will help to optimize the ICG delivery to tumors. Moreover, this study will also form the reference for studies involving ICG delivery to tumors using delivery systems such as nanoparticles. Overall this research will help in the efficient use ICG for tumor-diagnosis and anticancer therapy applications.

2. Materials and methods

2.1. Materials

ICG (free of sodium iodide) was obtained from Fisher Scientific (Fisher Scientific Inc., Pittsburgh, PA). Poly(DL-lactic-co-glycolic acid) 50:50 and polyvinyl alcohol (PVA) (88–89% hydrolyzed) were purchased from Sigma (Sigma Chemical Co., St. Louis, MO). All organic chemicals and solvents used were of reagent grade.

2.2. Animals

Pathogen free (healthy) C57BL/6 mice (female, 10-week old) were purchased from Taconic, Germantown, NY, housed and used according to the protocol approved by the university animal care committee.

2.3. Fluorescence spectroscopy instrumentation

The concentrations of ICG in various experiments were determined by a steady-state fluorescence technique using a K-2 fluorometer (ISS, Champaign, IL) equipped with a 70 mW cw diode laser. The diode laser has a wavelength of 786 nm, which was used as the excitation wavelength for all the experiments. Emission spectra were recorded from 795 to 845 nm.

2.4. Preparation and characterization of ICG-loaded PLGA nanoparticles

The ICG-loaded PLGA nanoparticles were prepared by a modified spontaneous emulsification solvent diffusion method and characterized according to our previous studies (Saxena et al., 2004a,c). ICG entrapment efficiency, ICG content and nanoparticle recovery were determined in triplicate by the steady-state fluorescence spectroscopy. Dynamic light scattering and atomic force microscopy was used for morphological characterization of nanoparticles. Nanoparticles were characterized with respect to zeta (ζ) potential by using zeta potential analyser. The release pattern of ICG from the nanoparticles was determined in phosphate buffer saline, PBS (pH 7.4) under sink conditions, in triplicate.

2.5. Preparation of free ICG solution and PLGA nanoparticles suspension

ICG stock solution of 100 μg/ml was freshly made just before the biodistribution studies, by dissolving 10 mg ICG in 100 ml of phosphate buffer saline (PBS) and PLGA nanoparticle stock suspension of 100 μg/ml was freshly made just before the biodistribution studies, by suspending PLGA nanoparticles (containing 10 mg of entrapped ICG) in 100 ml of PBS by sonication to get a homogenous suspension. Both stocks (free ICG solution and PLGA nanoparticle suspension) were used for all biodistribution studies. The stocks were further diluted with PBS to get the lower ICG concentrations.

2.6. Assay of ICG in biological samples

A fluorescence-based ICG assay was developed for analyzing ICG in the biological samples. ICG was first extracted from the samples. The tissue samples were homogenized with 20 volumes of DMSO, followed by a 4 h extraction (10 min for plasma samples) at room temperature in the dark. The mixtures were then centrifuged at 16,000 × g for 5 min. The concentration of ICG in the supernatant (containing the extracted ICG) was measured by steady-state fluorescence spectroscopy as described in Section 2.3, and then calculated according to a standard curve (extracts of ICG-free tissue homogenates and plasma were used as the background control). The tissue and plasma samples from the non-treated animal were also excited to measure the background fluorescence.

The extraction efficiency (recovery rate) was tested. For that, control (ICG-free) tissue and plasma samples were collected and

homogenized. Then the homogenate was spiked with a known quantity of ICG and mixed. After 1 h (10 min for plasma samples), the sample was extracted and analyzed according to the above procedure. The measured concentration was then compared to the added concentration.

2.7. In vivo biodistribution studies

For in vivo biodistribution studies, through the tail vein, a dose of 10 μg/200 μl of ICG either in free solution or in nanoparticle suspension was injected into each C57BL/6 mouse. The animals were euthanized and exsanguinated (three mice per time point for both dosage forms) at 5, 10, 15, 30, 45 and 60 min after the injection of free ICG solution and at 5, 10, 15, 30, 60, 120 and 240 min after the injection of nanoparticle suspension. The blood was collected and centrifuged to collect the plasma, while the liver, kidneys, lungs, heart and spleen were excised, rinsed, whipped and homogenized. The ICG content in the plasma and isolated organs were then assayed.

2.8. Statistical analysis

Data are expressed as mean ± S.D. Results of the in vivo biodistribution studies were evaluated by Student's *t*-test. Differences were considered significant at a level of $p < 0.05$.

3. Results and discussion

3.1. Characterization of nanoparticles

The following characterization of the nanoparticles was carried out according to our previous studies (Saxena et al., 2004a,c). The entrapment efficiency of ICG in PLGA nanoparticles was about 74.5 ± 2.2%, the ICG content of nanoparticles was 0.20 ± 0.01% (w/w) and nanoparticle recovery was about 45%. Mean diameter of the nanoparticles was 300 ± 10 nm with polydispersity index of 0.06. The nanoparticles obtained were nearly spherical in shape. The AFM image shows the numerous pores on the surface of the nanoparticles, which are responsible for the release of entrapped materials from the nanoparticles. The nanoparticles exhibited low zeta potential value of −16.3 mV. The release profile of ICG from the nanoparticles, under the sink conditions, is exponential, releasing 78% of ICG (within 8 h) followed by a slow release phase.

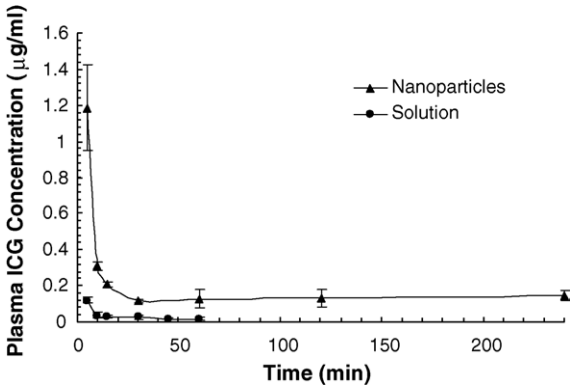

Fig. 1. ICG concentration–time course in mouse plasma after an i.v. dose of 10 μg ICG ($n = 3$).

3.2. Fluorescence assay suitability

The fluorescence signal from tissue and plasma samples, treated/spiked with ICG were ≥20 times higher than the signal from non-treated/unspiked samples, i.e. background (data not shown). This effect is due to the transparence of biomolecules in near-IR wavelengths, enabling fluorescence signals relatively free of intrinsic background interference. Thus, the fluorescence spectroscopy method used in this study is suitable for detection of ICG specifically.

3.3. Recovery of ICG from plasma and tissue samples

The extraction efficiency of ICG from the biological samples was determined by the analytical procedure described above. Since ICG does not metabolize in the body there is no interference due to any metabolites in its determination by the fluorometric method used (Paumgartner, 1975). As shown in Table 1, the recovery rates (efficiency of the extraction procedure) are in the range of 80–92% when the tissue and plasma drug concentration is within 0.01–1 μg/g of tissue. This recovery range is satisfactory for ICG assay in biological samples.

3.4. Biodistribution of ICG in mice through PLGA nanoparticles

In this study, the biodistribution of ICG in mice after single intravenous injection of ICG solution and ICG-loaded nanoparticles was investigated. Figs. 1–6 show the drug deposition in the

Table 1
Recovery (%) of ICG from mouse tissues and plasma for ICG solution and PLGA nanoparticles suspension (mean ± S.D., $n = 3$)

Concentration added (μg/g[a])	ICG solution			Nanoparticle suspension		
	1	0.1	0.01	1	0.1	0.01
Liver	83.4 ± 2.3	92.1 ± 3.7	85.3 ± 3.0	83.3 ± 4.0	84.4 ± 5.9	87.3 ± 6.1
Spleen	96.1 ± 3.9	95.8 ± 4.4	81.1 ± 3.8	89.5 ± 6.7	86.4 ± 5.2	80.7 ± 3.5
Lungs	95.2 ± 2.7	97.4 ± 5.9	81.1 ± 2.5	82.5 ± 4.1	82.7 ± 2.7	81.0 ± 5.1
Heart	100 ± 2.2	93.1 ± 6.3	80.0 ± 3.3	84.9 ± 5.1	83.5 ± 3.7	81.5 ± 6.2
Kidneys	89.3 ± 0.6	96.8 ± 4.9	91.1 ± 7.8	87.5 ± 5.5	82.3 ± 6.3	82.8 ± 5.6
Plasma	85.8 ± 2.3	87.9 ± 6.3	88.4 ± 4.4	82.1 ± 2.0	82.2 ± 3.8	80.8 ± 7.8

[a] μg/ml in case of plasma.

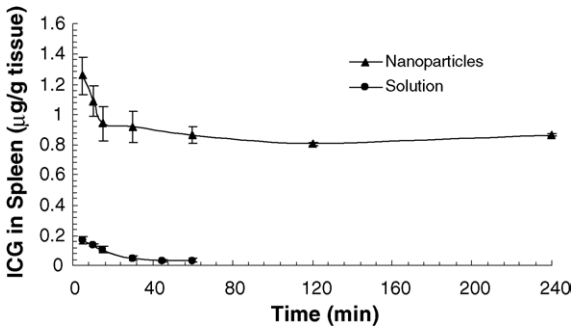

Fig. 2. ICG concentration–time course in mouse spleen after an i.v. dose of 10 μg ICG ($n = 3$).

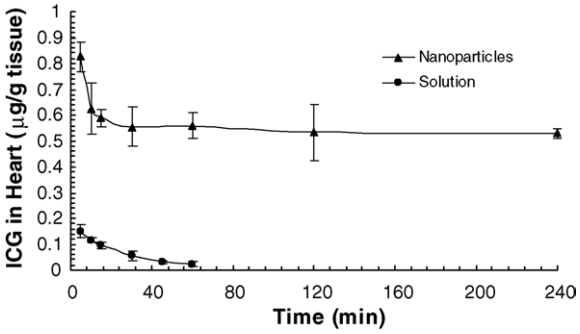

Fig. 3. ICG concentration–time course in mouse heart after an i.v. dose of 10 μg ICG ($n = 3$).

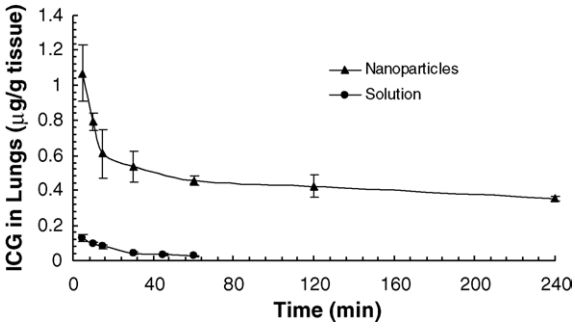

Fig. 4. ICG concentration–time course in mouse lungs after an i.v. dose of 10 μg ICG ($n = 3$).

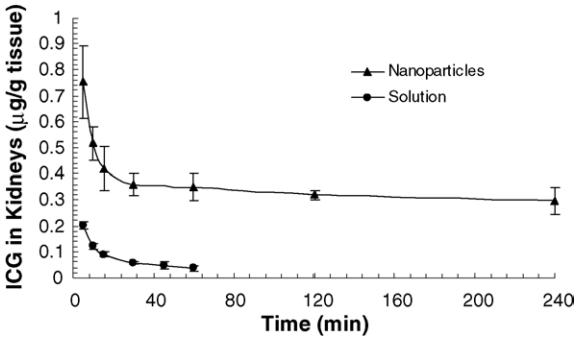

Fig. 5. ICG concentration–time course in mouse kidney after an i.v. dose of 10 μg ICG ($n = 3$).

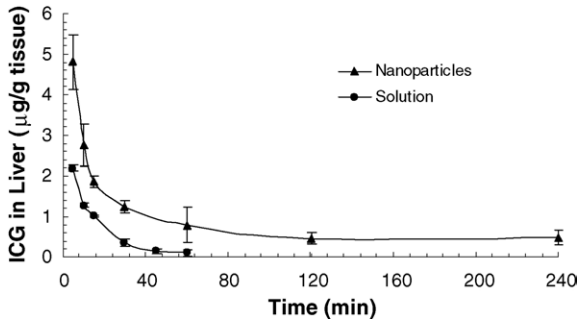

Fig. 6. ICG concentration–time course in mouse liver after an i.v. dose of 10 μg ICG ($n = 3$).

plasma, spleen, heart, lungs, kidneys and liver after intravenous injection of 10 μg ICG/mouse in solution or nanoparticle suspension.

The free solution form gave the highest ICG levels in the liver, followed by the kidneys, spleen, heart and lungs, indicating the major role of liver in the removal of ICG from the blood circulation followed by the kidneys. This observation is in accordance with the results reported by other authors (Paumgartner, 1975; Desmettre et al., 2000).

Whereas the nanoparticles formulation shows a different biodistribution pattern with highest ICG levels in the liver followed by spleen, lungs, heart and kidneys. As seen from Figs. 2–6 the major organs of removal for the nanoparticles are liver, lungs and spleen. Liver, lungs and spleen are the organs, which make the reticulo-endothelial system (RES) in the body (Monsky et al., 1999). Since, the RES is responsible for removing foreign particles from the blood circulation, the above observation is in accordance with the theory.

Interestingly, ICG concentration in the blood when delivered via nanoparticles was significantly higher (5–10 times) than when given as solution (Fig. 1). Moreover, when nanoparticles were used, the ICG concentration in the blood was significantly high till 4 h. This effect might be due to the relatively long circulation of the nanoparticles in the blood as compared to ICG solution or due to the controlled release of ICG from the nanoparticles deposited in various organs within the body. Further studies are needed to provide the complete explanation for such behavior. Moreover, the low amount of ICG present in the blood circulation when given in solution form was due to the fast removal of ICG by liver as shown in earlier studies (Paumgartner, 1975).

Also in all the organs, the ICG concentration was higher (from two to eight times) when delivered through nanoparticles as compared to ICG solution. This reflects higher uptake, accumulation and retention of ICG in various organs, when delivered through nanoparticles. This effect of nanoparticles might have occurred due the efficient nanoparticle-retention in the organs as compared to ICG solution. Further studies are required to prove the above concept.

As explained earlier in Section 1, the nanoparticles are targeted to the tumors by enhanced permeation and retention effect, which in turn is directly proportional to the time and amount of ICG in blood circulation. Thus, based on the results from

this study, it might be possible that when delivered through nanoparticles, more amount of ICG will be accumulated and retained in the tumors as compared to free ICG solution when a tumor-bearing animal model is used. At the same time, it might be possible that nanoparticle will enhance retention time and amount of ICG in the tumors since a tumor in the body also behaves as an organ with blood supplies. However, further studies with tumor-bearing animal models are required for proving the above hypothesis. Thus, the present study represents the first step in exploring the potential of nanoparticles as ICG-delivery system for use in tumor-diagnosis and photodynamic therapy.

4. Conclusions

A PLGA nanoparticulate delivery system for ICG was developed and characterized. The biodistribution of ICG when delivered through nanoparticles in healthy mice were determined using a fluorometric assay method. Compared to free solution, nanoparticles led to higher ICG deposit in organs (2–8 times) as well as in blood (5–10 times), reflecting the enormous potential of PLGA nanoparticles as delivery systems for ICG for its use in tumor-diagnosis and photodynamic therapy.

References

Abels, C., Fickweiler, S., Weiderer, P., Baumler, W., Hofstadter, F., Landthaler, M., Szeimies, R.M., 2000. Indocyanine green (ICG) and laser irradiation induced photooxidation. Arch. Dermatol. Res. 292, 404–411.

Desmettre, T., Devoisselle, J.M., Mordon, S., 2000. Fluorescence properties and metabolic features of indocyanine green (ICG) as related to angiography. Surv. Opthalmol. 45, 15–27.

Fickweiler, S., Szeimies, R.M., Baumler, W., Steinbach, P., Karrer, S., Goetz, A.E., Abels, C., Hofstadter, F., Landthaler, M., 1997. Indocyanine green: intracellular uptake and phototherapeutics effects in vitro. J. Photochem. Photobiol. B Biol. 38, 178–183.

Leroux, J.C., Doelker, E., Gurny, R., 1996. The use of drug-loaded nanoparticles in cancer chemotherapy. In: Benita, S. (Ed.), Microencapsulation: Methods and Industrial Applications. Marcel Dekker, New York, pp. 535–575.

Maarek, J.M.I., Holschneider, D.P., Harimoto, J., 2001. Fluorescence of indocyanine green in blood: intensity dependence on concentration and stabilization with sodium polyaspartate. J. Photochem. Photobiol. B Biol. 65, 157–164.

Monsky, W.L., Fukumura, D., Gohongi, T., Ancukiewcz, M., Weich, H.A., Torchilin, V.P., Yuan, F., Jain, R.K., 1999. Augmentation of transvascular transport of macromolecules and nanoparticles in tumors using vascular endothelial growth factor. Cancer Res. 59, 4129–4135.

Mordon, S., Devoisselle, J.M., Soulie-Begu, S., Desmettre, T., 1998. Indocyanine green: physicochemical factors affecting its fluorescence in vivo. Microvasc. Res. 55, 146–152.

Paumgartner, G., 1975. The handling of indocyanine green by the liver. Schweiz. Med. Wochenschr. 105, 1–30.

Philip, R., Penzkofer, A., Baumler, W., Szeimies, R.M., Abels, C., 1996. Absorption and fluorescence spectroscopic investigation of indocyanine green. J. Photochem. Photobiol. A Chem. 96, 137–148.

Saxena, V., Sadoqi, M., Shao, J., 2003. Degradation kinetics of indocyanine green in aqueous solution. J. Pharm. Sci. 92, 2090–2097.

Saxena, V., Sadoqi, M., Shao, J., 2004a. Enhanced photo-stability, thermal-stability and aqueous-stability of indocyanine green in polymeric nanoparticulate systems. J. Photochem. Photobiol. B Biol. 74, 29–38.

Saxena, V., Sadoqi, M., Kumar, S., Shao, J., 2004b. Tiny bubbles. SPIE's OE Mag. 4, 21–23.

Saxena, V., Sadoqi, M., Shao, J., 2004c. Indocyanine green loaded biodegradable nanoparticles: preparation, physicochemical characterization and in-vitro release. Int. J. Pharm. 278, 293–301.

Saxena, V., Sadoqi, M., Shao, J., Kumar, S., 2005. Enhanced intracellular uptake of indocyanine green by polymeric nanoparticulate delivery systems. J. Biomed. Nanotechnol. 1, 168–175.